Article **Journal Renewable Energy**
June, 2023 Vol.7 No.18 1-8

Design of a p-i-n type inverted perovskite solar cell using SiO_x as down-conversion material to improve PCE: Simulation and optimization in SCAPS-1D

Diseño de una celda solar de perovskita tipo p-i-n utilizando SiO_x como material de energía de conversión descendente para mejorar el PCE: Simulación y optimización en SCAPS-1D

PAZ-TOTOLHUA, Ezequiel[1]†*, CARRILLO-LÓPEZ, Jesús[1], LUNA-LÓPEZ, José Alberto[1] and BENÍTEZ-LARA, Alfredo[2]

[1]*Benemérita Universidad Autónoma de Puebla, Centro de Investigaciones en Dispositivos Semiconductores (CIDS-ICUAP), Av. San Claudio y 14 sur, Edificios IC5 y IC6, C. U., Col. San Manuel, Puebla, Pue. 72570, México.*
[2]*Centro de Investigaciones en Óptica A.C., Lomas del Bosque 115, León, Guanajuato. 37150, México.*

ID 1st Autor: *Ezequiel, Paz-Totolhua* / **ORC ID:** 0000-0001-6826-5353, **CVU CONAHCYT ID**: 712701

ID 1st Co-author: *Jesús, Carrillo-López* / **ORC ID:** 0009-0002-9036-6999, **CVU CONAHCYT ID**: 5242

ID 2nd Co-author: *Jose Alberto, Luna-López* / **ORC ID:** 0000-0002-7647-3184, **CVU CONAHCYT ID**: 200808

ID 3rd Co-author: *Alfredo, Benítez-Lara* / **ORC ID:** 0000-0002-7206-2767, **CVU CONAHCYT ID**: 256851

DOI: 10.35429/JRE.2023.18.7.1.8 Received March 16, 2023; Accepted June 30, 2023

Abstract

In this research work, an inverted p-i-n type perovskite solar cell: ITO/PEDOT: PSS/$CH_3NH_3PbI_3$/PCBM/Au has been simulated and optimized in SCAPS-1D. The optimized parameters in SCAPS-1D that improved solar performance were: perovskite thickness, the total defect density of perovskite, the total defect density of interfaces, series and shunt resistances, and device operating temperature. As a result, the efficiency (PCE) increased to 18.33%. Subsequently, when the silicon-rich oxide (SiOx) material was implemented in the simulation as down-conversion energy material on the outside of the cell, a power conversion efficiency (PCE) of 23.7% was obtained. The SiO_X film obtained experimentally by sputtering obtained good photoluminescence, absorption coefficient, band gap, and transmittance characteristics before and after thermal annealing. These characteristics have been considered for the proposed device. It is indicated that the inverted perovskite solar cell of type p-i-n: SiO_x/ITO/PEDOT:PSS/$CH_3NH_3PbI_3$/PCBM/Au has better J-V output values and EQ quantum efficiency than the perovskite solar cell without SiOx.

Perovskite, Efficiency, Simulated

Resumen

En este trabajo de investigación, una celda solar de perovskita tipo p-i-n invertida: ITO/PEDOT: PSS/$CH_3NH_3PbI_3$/PCBM/Au ha sido simulada y optimizada en el software SCAPS-1D. Los parámetros optimizados en SCAPS-1D que mejoraron el rendimiento solar fueron: el grosor de la perovskita, la densidad total de defectos de la perovskita, la densidad total de defectos de las interfaces, las resistencias en serie y derivación y la temperatura de operación del dispositivo. Como resultado de esto, la eficiencia (PCE) incrementó a 18.33%. Posteriormente, cuando se implementó en la simulación el óxido rico en silicio (SiOx) como material de energía de conversión descendente en la parte externa de la celda, se obtuvo una eficiencia (PCE) de 23.7 %. La película de SiO_X obtenida experimentalmente por sputtering obtuvo buenas características de fotoluminiscencia, coeficiente de absorción, band gap y transmitancia antes y después del recocido térmico. Estas características fueron consideraras en el dispositivo propuesto. Se concluye que la celda solar de perovskita: SiO_x/ITO/PEDOT: PSS/$CH_3NH_3PbI_3$/PCBM/Au tiene mejores valores de salida J-V y eficiencia cuántica EQ que la celda solar sin SiO_x.

Perovskita, Eficiencia, Simulado

Citation: PAZ-TOTOLHUA, Ezequiel, CARRILLO-LÓPEZ, Jesús1, LUNA-LÓPEZ, José Alberto and BENÍTEZ-LARA, Alfredo. Design of a p-i-n type inverted perovskite solar cell using SiOx as down-conversion material to improve PCE: Simulation and optimization in SCAPS-1D. Journal Renewable Energy. 2023. 7-18: 1-8

*Correspondence to Author (e-mail: ezequiel.paz@alumno.buap.mx)
† Researcher contributing as first author.

Introduction

Perovskite solar cells (PSCs) have become a principal source of research since their emergence in 2009. They are currently the most promising devices of the future for use as a renewable energy source. In just a few years, they have made remarkable progress as their efficiency has been certified up to 25.5 %, comparable to silicon (Si), gallium arsenide (GaAs), and cadmium telluride (CdTe) technology, according to Chao *et al*., (2021). Until now, most perovskite solar cells (PSCs) have been fabricated with the traditional vertical or n-i-p type structure. Notwithstanding, these devices suffer from severe hysteresis effects and have poor stability. In contrast, the inverted or p-i-n type cell has good, fewer defective states between interfaces it is possible to fabricate devices at low temperatures (Yang *et a*l., 2022).

Notwithstanding, metal-organic perovskite ($CH_3NH_3PbI_3$) remains one of the materials used in perovskite solar cells due to its simple synthesis process, low cost, and high performance (Yin *et al*., 2022). Nevertheless, its instability and easy degradation due to environmental factors are still an obstacle to its commercialization (Mazumdar *et al*., 2021). Perovskite $CH_3NH_3PbI_3$ has many advantages as a high absorption coefficient, tunable band gap, high charge carrier mobility, low trap density, long carrier diffusion length, and small exciton binding energy (Mohanty *et al*., 2019).

Researchers are exploring a lot in the field of perovskites as the use of different structures in solar cells, the design of new hole and electron transport materials, the improvement of perovskite materials, and the implementation of interlayers to achieve higher efficiency and improved spectral response. Improving the utilization of the incident solar spectrum may be one of the approaches to increase the performance of these devices because currently, perovskite solar cells can only utilize a fraction of the incident solar photons, ranging from the visible to the near infrared (Datt, Bishnoi, Lee, *et al*., 2022). That is ultraviolet (UV) regions are not used and are considered harmful.

According to the literature, a down-conversion energy material absorbs the short wavelength photons of the solar spectrum, which the solar cell does not use efficiently, and re-emits them at longer wavelengths (Hosseini & Ghanbari, 2018). The main characteristics of a down-conversion energy material are high photoluminescence quantum efficiency (PLQE), photochemical and environmental stability, broadband absorption in the region where the spectral response of the solar cell is low, high absorption coefficient in low wavelength region, high transmittance and broadband emission, particularly in the region where the device response is high, sufficient stokes shift to minimize the self-absorption energy losses due to the spectral overlap between the absorption and emission bands, low cost, easy to process and can be deposited by the large scalable method, and low film roughness (Datt, Bishnoi, Hughes, *et al*., 2022).

An alternative to solve spectral mismatch losses, improve stability, and increase efficiency is to apply a silicon-rich oxide (SiO_x) layer on the surface of a perovskite solar cell. This material is a silicon oxide out of stichometry that contains small silicon islands embedded in a silicon dioxide matrix and stands out for its high photoluminescence intensity of red light when illuminated with ultraviolet UV radiation (Vivaldo *et al*., 2016).

In this work, the photovoltaic characteristics of a SiOx film deposited by co-sputtering have been reviewed for implementation in perovskite solar cells. Subsequently, an inverted perovskite solar cell type p-i-n: ITO/PEDOT: PSS/$CH_3NH_3PbI_3$/PCBM/Au was numerically simulated. Photovoltaic parameters such as perovskite thickness, total defect densities, series and shunt resistances, and operating temperature were optimized for this device, reaching an efficiency of 18.33 %. The J-V output values were compared with those reported experimentally. Finally, a new device model was proposed: SiO_x/ITO/PEDOT: PSS/$CH_3NH_3PbI_3$/PCBM/Au, which includes a down-conversion energy material (SiO_x) on the outside, and whose efficiency increased to 23.74 %. In the latter simulation, the J-V output characteristics and QE quantum efficiency were better than those of the device without SiO_x.

ISSN 2523-2881

PAZ-TOTOLHUA, Ezequiel, CARRILLO-LÓPEZ, Jesús1, LUNA-LÓPEZ, José Alberto and BENÍTEZ-LARA, Alfredo. Design of a p-i-n type inverted perovskite solar cell using SiOx as down-conversion material to improve PCE: Simulation and optimization in SCAPS-1D. Journal Renewable Energy. 2023

Numerical methodology

Solar cell structure

The simulated inverted perovskite solar cell has the configuration ITO/PEDOT: PSS/$CH_3NH_3PbI_3$/PCBM/Au, where indium doped tin oxide (ITO) is the front contact; poly (3,4- ethylenedioxythiophene) polystyrene sulfonate (PEDOT: PSS) is the hole transport layer; $CH_3NH_3PbI_3$ is the absorber layer; Phenyl-C61-butyric acid and methyl ester (PCBM) is the electron transport layer; and gold (Au) is the back metal contact. In addition to the proposed model SiO_x/ITO/PEDOT/$CH_3NH_3PbI_3$/PCBM/Au is a device that includes an outer layer of silicon-rich oxide (SiO_x), which works as a down-conversion energy material. The two solar structures are represented in Figure 1 (a, b) and the energy band diagram is shown in Figure 1 (c).

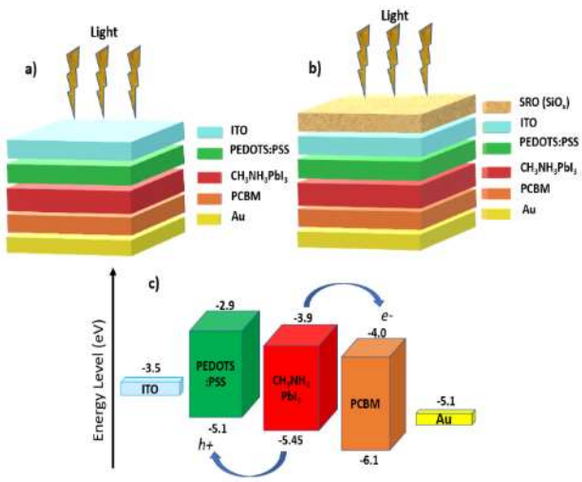

Figure 1 (a) Schematic diagram of perovskite solar cell; (b) Schematic diagram of perovskite solar cell with SiO_x; (c) Energy band gap diagram
Source: Own elaboration, Paint 3D

Numerical method

The simulation was performed in SCAPS-1D software version 3.3.10 under AM1.5G illumination at 300 K ambient temperature. The SCAPS-1D software, developed at the Department of Electronics and Information Systems (ELIS) at the University of Ghent in Belgium, has been used to model and simulate solar cells (Burgelman *et al*., 2000). The software solves the semiconductor equations in one dimension in a steady state (Decock *et al*., 2013) and (Burgelman *et al*., 2013).

The main equations it solves are the Poisson equation (1), the electron continuity equation (2), the hole continuity equation (3), the electron charge transport equation (4), the hole charge transport equation (5), and the absorption coefficient (6), which are solved until convergence occurs (Verschraegen & Burgelman, 2007).

Poisson equation:

$$\frac{dE}{dx} = \frac{q}{\varepsilon_0 \varepsilon_r}[p(x) - n(x) + N_D^+(x) - N_A^-(x) + p_t(x) - n_t(x)] \quad (1)$$

Where E is the electric field, q is electronic charge, ε_0 is permittivity of vacuume, ε_r is relative permittivity, N_D^+ is the shallow donor impurity density, $N_A^+$is the shallow aceptor impurity density, $n(x)$ and $p(x)$ are the densities of electrons and holes. Similarly $p_t(x)\ y\ n_t(x)$represent the trapped holes and electrons as a function of x respectively.

Continuity equations:

$$\frac{dJ_n}{dx} = G - U_n \quad (2)$$

$$\frac{dJ_p}{dx} = G - U_p \quad (3)$$

Where J_n and J_p are the electron and hole current densities, G is the generation rate, U_n and U_p are the recombination rates for electrons and holes respectively.

Charge transport equation:

$$J_n = D_n \frac{dn}{dx} + \mu_n n \frac{d\phi}{dx} \quad (4)$$

$$J_p = D_p \frac{dp}{dx} + \mu_p p \frac{d\phi}{dx} \quad (5)$$

Where $D_n$and $D_p$are the electron and hole diffusion coefficients respectively, μ_n and μ_p are the electron and hole mobility respectively.

Absorption coefficient equation:

$$\alpha(\lambda) = (A + \frac{B}{h\nu})\sqrt{h\nu - E_g} \quad (6)$$

Where $A$and B are constants, h is Planck constant, ν is frequency of photon and E_g is the band gap of the absorber layer.

ISSN 2523-2881

Simulation parameters

The physical, optical, and electrical parameters were obtained from the scientific literature and summarized in Table 1 (Basyoni *et al*., 2021; A. Ghosh *et a*l., 2020; B. Ghosh *et al*., 2022; Jamal *et a*l., 2019; Sabbah *et al*., 2022). The parameters used for the silicon-rich oxide SiO_x correspond to a SiO_2 film. Nevertheless, the absorption coefficient, the photoluminescence, and the band gap are the results of the characterization of the deposits obtained by co-sputtering for this work. In addition, the work function for the metal contact (Au) was 5.1 eV.

Photovoltaic Parameters	SiOx	ITO	PEDOTS: PSS	$CH_3HN_3PbI_3$	PCBM
Thickness (nm)	90	100	40	300	80
Energy Band gap, *Eg* (eV)	4.5	3.5	2.2	1.57	2.1
Electron affinity, χ (eV)	0.950	2.3	2.9	3.9	4.1
Dielectric permittivity, *εr*	3.9	9	2.3	18	4
Effective Density of stated at conduction band, *Nc* ($1/cm^3$)	2.8×10^{18}	2.2×10^{18}	2.2×10^{18}	2.2×10^{18}	2.5×10^{19}
Effective Density of stated at valence band, *Nv* ($1/cm^3$)	2.6×10^{19}	1.8×10^{19}	2.8×10^{18}	1.9×10^{19}	2.5×10^{19}
Electron thermal velocity, Vh (cm/s)	1×10^7	1×10^7	1×10^7	1×10^7	1×10^7
Hole thermal velocity, Ve (cm/s)	1×10^7	1×10^7	1×10^7	1×10^7	1×10^7
Hole mobility, *μn* (cm^2/Vs)	1.5×10^3	31	0.0002	3	0.01
Electron Mobility, *μp* (cm^2/Vs)	4.5×10^3	50	0.02	17	0.01
Uniform Shallow Donor Dopping, N_D ($1/cm^3$)	0	0	0	0	5×10^{17}
Uniform Shallow Acceptor Dopping, N_A ($1/cm^3$)	2.0×10^{18}	2.0×10^{16}	1×10^{18}	0	0
Defect density, *Nt* ($1/cm^3$)	10^{15}	10^{15}	10^{15}	10^{15}	10^{15}

Table 1 Optical and electrical parameters for simulation
Source: Own elaboration, summary of bibliography

Figure 2 shows the definition and editing panel in the SCAPS-1D software. In this section, you can enter and edit the electrical and optical parameters of the layers, the direction of light incidence, and the interface parameters.

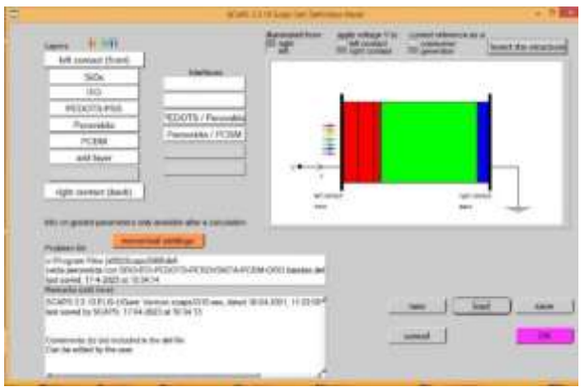

Figure 2 Definition and editing panel in the SCAPS-1D simulator
Source: SCAPS-1D Software version 3.3.10

Results and discusión

Photoluminescence, absorption coefficient, band gap, and transmittance of SiO_x

The silicon-rich oxide (SiO_x) film was deposited by co-sputtering on 1" x 1" x 1 mm quartz substrates, obtaining a thickness of 90 nm with low roughness. The SiO_x film was deposited by simultaneous sputtering of Si and SiO_2 targets. The equipment used for the deposition was a magnetron sputtering system. The deposition parameters were estimated to reach an average silicon excess (5.9 at. %) to achieve a maximum photoluminescence emission in the red region, according to Coyopol *et al*., (2018).

Graph 1 shows the PL photoluminescence spectrum, where it is observed that SiO_x has PL emission in the red-blue region before and after thermal annealing. SiO_x before annealing shows a dominant emission peak at 423 nm, with two smaller peaks at 640 nm and 780 nm after deconvolution. After thermal annealing at 1100°C for 2 hours, the film obtained two emission peaks, one in the red region (775 nm) and another of lower intensity in the blue region (418 nm). The PL emission peaks are associated with the complete activation of Si=O defects, favored by the average size of silicon nanocrystals embedded in a silicon-rich oxide dielectric matrix (Coyopol *et al*., 2016).

ISSN 2523-2881

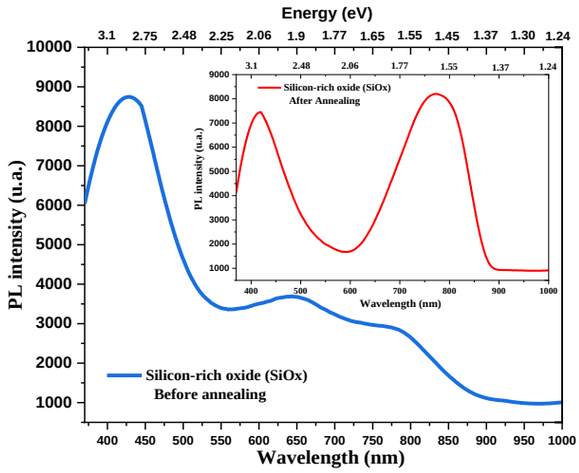

Graph 1 Photoluminescence spectra of silicon-rich oxide (SiO_x) before and after thermal annealing
Source: Own elaboration, OriginPro 2018

Graph 2 shows the absorption coefficient and band gap obtained from the SiO_x film after thermal annealing. The graph shows that the film has a high absorption coefficient in the low wavelength region (ultraviolet UV). In addition, the film has a low absorption coefficient in the range from 350 nm to 800 nm, which corresponds to the visible spectrum.The band gap energy was estimated using the Tauc relation and the Beer Lambert equation. This absorption coefficient and the band gap have been used in the SCAPS-1D simulator.

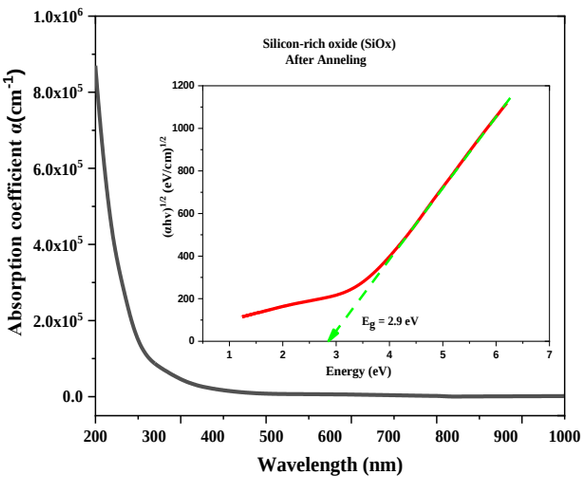

Graph 2 Absorption coefficient of silicon-rich oxide (SiOx)
Source: Own elaboration, OriginPro 2018

Graph 3 shows the transmittance spectrum of the SiO_x film after thermal annealing. The graph shows that the film has a transmittance above 90% in the range from 400 nm to 800 nm, which is the visible spectrum.

In addition, the film shows a progressive decrease in transmittance in the 200 nm to 400 nm range, which corresponds to the ultraviolet spectrum. These results agree with the absorption coefficient, concluding that the spectral response of the SiO_x film is concentrated in the ultraviolet region.

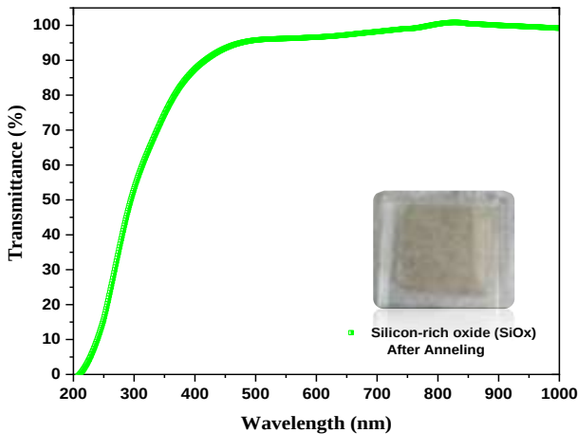

Graph 3 Transmittance spectrum of silicon-rich oxide (SiO_x)
Source: Own elaboration, OriginPro 2018

J-V current-voltage curve, EQ quantum efficiency, and band diagram

This section shows the J-V plot, QE quantum efficiency plot, and energy band diagram of the perovskite solar cell: ITO/PEDOT:PSS/$CH_3NH_3PbI_3$/PCBM/Au and the proposed perovskite solar cell: SiO_x/ITO/PEDOT:PSS/$CH_3NH_3PbI_3$/PCBM/Au. Furthermore, we have considered the optimum values obtained from the SCAPS-1D simulation. Table 2 shows the optimal values for perovskite thickness, total defect density, series and shunt resistance, and solar cell operating temperature. The parameters were varied in the simulator, keeping the other parameters constant.

Parameters	Variation range	Optimal value
Perovskite thickness	50-1000 nm	500 nm
Perovskite defect density	10^{10}-10^{20} cm^{-3}	10^{13} cm^{-3}
Defect density of PEDOTS:PSS/Perovskite interface	10^{10}-10^{20} cm^{-3}	10^{13} cm^{-3}
Defect density of Perovskite/PCBM interface	10^{10}-10^{20} cm^{-3}	10^{13} cm^{-3}
Series Resistance	10-100 $\Omega.cm^2$	10 $\Omega.cm^2$
Shunt Resistance	500-5000 $\Omega.cm^2$	5000 $\Omega.cm^2$
Operating temperature of the solar cell	300-390 K	300 K

Table 2 Optimal values obtained from SCAPS-1D
Source: Own Elaboration

ISSN 2523-2881

Simulation of the perovskite solar cell: ITO/PEDOT: PSS/$CH_3NH_3PbI_3$/PCBM/Au produced output values of Voc = 1.112 V, Jsc =20.236 mA/cm^2, FF = 81.24 % and PCE =18.33 %, similar to those reported experimentally, according to Heo *et al*., (2015).

Notwithstanding, the proposed perovskite solar cell:SiO_x /ITO/PEDOT:PSS/$CH_3NH_3PbI_3$/PCBM/Au, containing a SiO_x monolayer film, produced output values of Voc = 1.088 V, Jsc =27.236 mA/cm^2, FF = 80.06 % and PCE = 23.74 %. Graph 4 shows the J-V curves with the output values of both devices.

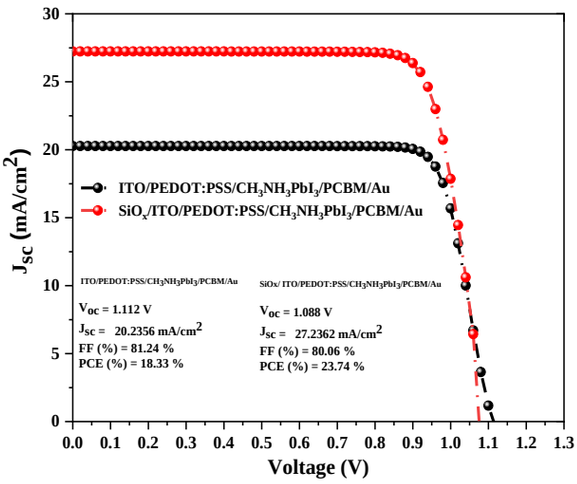

Graph 4 J-V curve of perovskite solar cell with and without SiO_x
Source: Own Elaboration, OriginPro 2018

Graph 5 shows the QE quantum efficiency for both devices. An improvement in the QE quantum efficiency is observed for the solar cell that includes the SiO_x film compared to the one that does not. The range of enhancement is observed mainly in the wavelength range from 500 to 780 nm. This increase determines that the structure with the SiO_x film has a better spectral response.

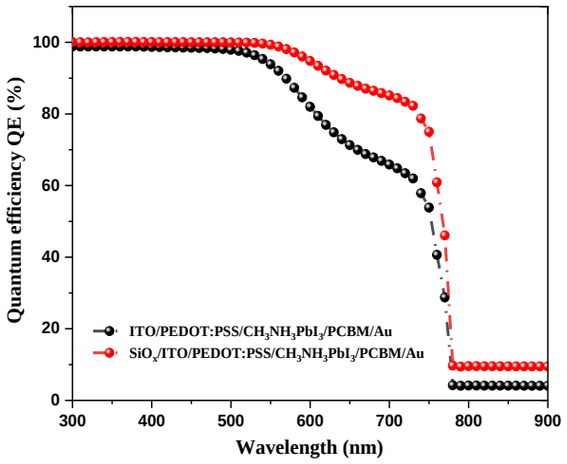

Graph 5 QE Quantum efficiency of perovskite solar cell with and without SiO_x
Source: Own Elaboration, OriginPro 2018

Graph 6 shows the band diagram of the perovskite solar cell with the optimized parameters and the SiO_x down-conversion material. It is observed that there is a splitting of the valence band and conduction band. In addition, the energy band diagram indicates that both the PEDOTS: PSS material and the PCBM material have higher energy bandwidths compared to the absorber layer ($CH_3NH_3PbI_3$), so there is a band alignment, favoring the passage of electrons and holes generated in the perovskite. Meanwhile, the energy barriers at the interfaces ensure the diffusion of carriers generated in the perovskite into the hole and electron transport layers. Finally, the transparent SiO_x material filters visible light due to its wide band gap and, at the same time, absorbs ultraviolet light, which contributes to increasing the photocurrent.

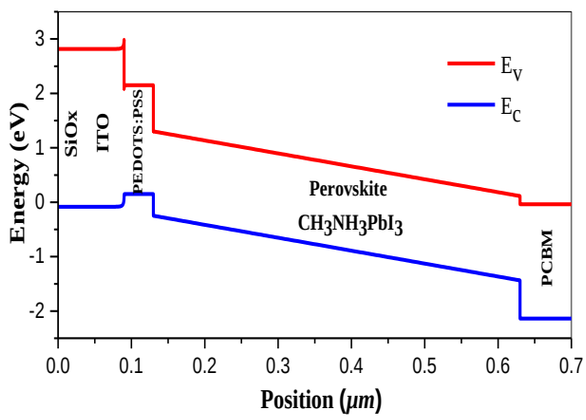

Graph 6 Energy band diagram of perovskite solar cell with SiO_x
Source: Own Elaboration, OriginPro 2018 and SCAPS-1D

ISSN 2523-2881

Acknowledgments

The authors thank the laboratories of INAOE, CIMAV, CIO, and CIDS-BUAP for their help in obtaining and characterizing the samples.

Funding

This work has been funded by CONAHCYT [grant number: 712701].

Conclusions

A p-i-n type inverted perovskite solar cell: ITO/PEDOT:PSS/$CH_3NH_3PbI_3$/PCBM/Au has been simulated and optimized in SCAPS-1D software.

The optimal values obtained from the simulation indicate that a perovskite layer thickness of 500 nm, a total defect density at the perovskite and interfaces of 10^{13} cm^{-3}, a series and shunt resistance of 10 $\Omega.cm^2$ and 5000 $\Omega.cm^2$ respectively, and an operating temperature of 300 K improve the performance of the solar cell.

In addition, the experimentally obtained silicon-rich oxide (SiOx) material has the main characteristics of an energy down-conversion material for application in perovskite solar cells. In conclusion, the solar device: SiOx/ITO/PEDOT:PSS/$CH_3NH_3PbI_3$/PCBM/Au has the potential to generate a higher photocurrent, as the simulation results in an improved efficiency of 23.74 %, while the solar device without the SiOx film: ITO/ PEDOT:PSS/$CH_3NH_3PbI_3$/PCBM/Au produces an efficiency of 18.33 %, slightly higher than the experimental data, i.e. 18.1 %. The perovskite solar cell with SiOx is considered efficient, as it has a simple architecture in addition to the fact that it can easily obtain experimental verification.

References

Basyoni, M. S. S., Salah, M. M., Mousa, M., Shaker, A., Zekry, A., Abouelatta, M., Alshammari, M. T., Al-Dhlan, K. A., & Gontrand, C. (2021). On the Investigation of Interface Defects of Solar Cells: Lead-Based vs Lead-Free Perovskite. *IEEE Access*, *9*, 130221–130232. https://doi.org/10.1109/ACCESS.2021.3114383

Burgelman, M., Decock, K., Kheli, S., & Abass, A. (2013). Advanced electrical simulation of thin film solar cells. *Thin Solid Films*, *535*, 296–301. https://doi.org/doi:10.1016/j.tsf.2012.10.032

Burgelman, M., Nollet, P., & Degrave, S. (2000). Modelling polycrystalline semiconductor solar cells. *Thin Solid Films*, *361*, 527–532. https://doi.org/doi:10.1016/s0040-6090(99)00825-1

Chao, L., Niu, T., Gao, W., Ran, C., Song, L., Chen, Y., & Huang, W. (2021). Solvent Engineering of the Precursor Solution toward Large-Area Production of Perovskite Solar Cells. *Advanced Materials*, *33*(14), 1–23. https://doi.org/10.1002/adma.202005410

Coyopol, A., Cardona, M. A., Díaz Becerril, T., Licea Jimenez, L., & Morales Sánchez, A. (2016). Silicon excess and thermal annealing effects on structural and optical properties of co-sputtered SRO films. *Journal of Luminescence*, *176*, 40–46. https://doi.org/10.1016/j.jlumin.2016.02.033

Coyopol, A., Díaz, T., Garcia, G., Cabañas, S., Palacios, L., & Morales, A. (2018). Synthesis and Luminescent Properties of Silicon Nanocrystals. *IntechOpen*, *11*(tourism), 13. https://doi.org/http://dx.doi.org/10.5772/intechopen.74286

Datt, R., Bishnoi, S., Hughes, D., Mahajan, P., Singh, A., Gupta, R., Arya, S., Gupta, V., & Tsoi, W. C. (2022). Downconversion Materials for Perovskite Solar Cells. *Solar RRL*, *2200266*, 2200266. https://doi.org/10.1002/solr.202200266

Datt, R., Bishnoi, S., Lee, H. K. H., Arya, S., Gupta, S., Gupta, V., & Tsoi, W. C. (2022). Down- conversion materials for organic solar cells: Progress, challenges, and perspectives. *Aggregate*, *3*(3), 1–21. https://doi.org/10.1002/agt2.185

Decock, K., Khelifi, S., & Burgelman, M. (2013). Modelling and measurement of the metastable defect distribution in chalcopyrite-based thin film solar cells. *Thin Solid Films*, *535*(1), 362–365. https://doi.org/10.1016/j.tsf.2012.10.078

Ghosh, A., Dipta, S., Nikor, S., Saqib, N., & Saha, A. (2020). Performance analysis of an efficient and stable perovskite solar cell and a comparative study of incorporating metal oxide transport layers. *Journal of the Optical Society of America B*, *37*(7), 1966. https://doi.org/10.1364/josab.391817

Ghosh, B., Nasir, S., Chee, F., Routray, S., Saad, I., & Mohamad, K. (2022). Numerical study of nSi and nSiGe solar cells: Emerging microstructure nSiGe cell achieved the highest 8.55% efficiency. *Optical Materials*, *129*(June), 6. https://doi.org/10.1016/j.optmat.2022.112539

Heo, J. H., Han, H. J., Kim, D., Ahn, T. K., & Im, S. H. (2015). Hysteresis-less inverted CH3NH3PbI3 planar perovskite hybrid solar cells with 18.1% power conversion efficiency. *Energy and Environmental Science*, *8*(5), 1602–1608. https://doi.org/10.1039/c5ee00120j

Hosseini, Z., & Ghanbari, T. (2018). Designing an efficient graphene quantum dot-filled luminescent down shifting layer to improve the stability and efficiency of perovskite solar cells by simple optical modeling. *RSC Advances*, *8*(55), 31502–31509. https://doi.org/10.1039/c8ra06196c

Jamal, M. S., Shahahmadi, S. A., Chelvanathan, P., Asim, N., Misran, H., Hossain, M. I., Amin, N., Sopian, K., & Akhtaruzzaman, M. (2019). Effect of defect density and energy level mismatch on the performance of perovskite solar cells by numerical simulation. *Optik*, *182*, 1204–1210. https://doi.org/10.1016/j.ijleo.2018.12.163

Mazumdar, S., Zhao, Y., & Zhang, X. (2021). Stability of Perovskite Solar Cells: Degradation Mechanisms and Remedies. *Frontiers in Electronics*, *2*(August), 1–34. https://doi.org/10.3389/felec.2021.712785

Mohanty, I., Mangal, S., Jana, S., & Singh, U. P. (2019). Stability factors of perovskite (CH3NH3PbI3) thinfilms for solar cell applications: A study. *Materials Today: Proceedings*, *39*(July 2021), 1829–1832. https://doi.org/10.1016/j.matpr.2020.06.183

Sabbah, H., Arayro, J., & Mezher, R. (2022). Simulation and Investigation of 26% Efficient and Robust Inverted Planar Perovskite Solar Cells Based on GA0.2FA0.78SnI3-1%EDAI2 Films. *Nanomaterials*, *12*(21), 1–19. https://doi.org/10.3390/nano12213885

Verschraegen, J., & Burgelman, M. (2007). Numerical modeling of intra-band tunneling for heterojunction solar cells in scaps. *Thin Solid Films*, *515*(15 SPEC. ISS.), 6276–6279. https://doi.org/10.1016/j.tsf.2006.12.049

Vivaldo, I., Carrillo, J., López, O., Jiménez, S., Martínez, J., Murias, D., & López, J. A. (2016). Study of the photon down-conversion effect produced by thin silicon-rich oxide films on silicon solar cells. *INTERNATIONAL JOURNAL OF ENERGY RESEARCH*, *33*(4), 23–40. https://doi.org/10.1002/er

Yang, J., Luo, X., Zhou, Y., Li, Y., Qiu, Q., & Xie, T. (2022). Recent Advances in Inverted Perovskite Solar Cells: Designing and Fabrication. *International Journal of Molecular Sciences*, *23*(19). https://doi.org/10.3390/ijms231911792

Yin, Z., Lu, B., Chen, Y., & Guo, C. (2022). Advances of Commercial and Biological Materials for Electron Transport Layers in Biological Applications. *Frontiers in Bioengineering and Biotechnology*, *10*(May), 1–20. https://doi.org/10.3389/fbioe.2022.900269

ISSN 2523-2881